

Novel structural templates for estrogen-receptor ligands and prospects for combinatorial synthesis of estrogens

Brian E Fink, Deborah S Mortensen, Shaun R Stauffer, Zachary D Aron and John A Katzenellenbogen

Introduction: The development of estrogen pharmaceutical agents with appropriate tissue-selectivity profiles has not yet benefited substantially from the application of combinatorial synthetic approaches to the preparation of structural classes that are known to be ligands for the estrogen receptor (ER). We have developed an estrogen pharmacophore that consists of a simple heterocyclic core scaffold, amenable to construction by combinatorial methods, onto which are appended 3–4 peripheral substituents that embody substructural motifs commonly found in nonsteroidal estrogens. The issue addressed here is whether these heterocyclic core structures can be used to prepare ligands with good affinity for the ER.

Results: We prepared representative members of various azole core structures. Although members of the imidazole, thiazole or isoxazole classes generally have weak binding for the ER, several members of the pyrazole class show good binding affinity. The high-affinity pyrazoles bear close conformational relationship to the nonsteroidal ligand raloxifene, and they can be fitted into the ligand-binding pocket of the ER–raloxifene X-ray structure.

Conclusions: Compounds such as these pyrazoles, which are novel ER ligands, are well suited for combinatorial synthesis using solid-phase methods.

Address: Department of Chemistry, University of Illinois, 600 S. Mathews Avenue, Urbana, IL 61801, USA.

Correspondence: John A Katzenellenbogen
E-mail: jkatzene@uiuc.edu

Key words: arylpyrazoles, combinatorial chemistry, estrogen receptor, estrogen ligands, nonsteroidal estrogens

Received: 16 November 1998
Revisions requested: 15 December 1998
Revisions received: 20 January 1999
Accepted: 28 January 1999

Published: 18 March 1999

Chemistry & Biology April 1999, 6:205–219
<http://biomednet.com/elecref/1074552100600205>

© Elsevier Science Ltd ISSN 1074-5521

Introduction

Estrogens are endocrine regulators of the vertebrate reproductive system that have important effects in many non-reproductive tissues as well (bone, liver, cardiovascular system, CNS and so on). Many estrogen pharmaceuticals, based on both natural and synthetic substances, have been developed as agents for regulating fertility, preventing and controlling hormone-responsive breast cancer, and menopausal hormone replacement. These substances display a spectrum of agonist to antagonist activity that can show remarkable tissue and cell selectivity [1].

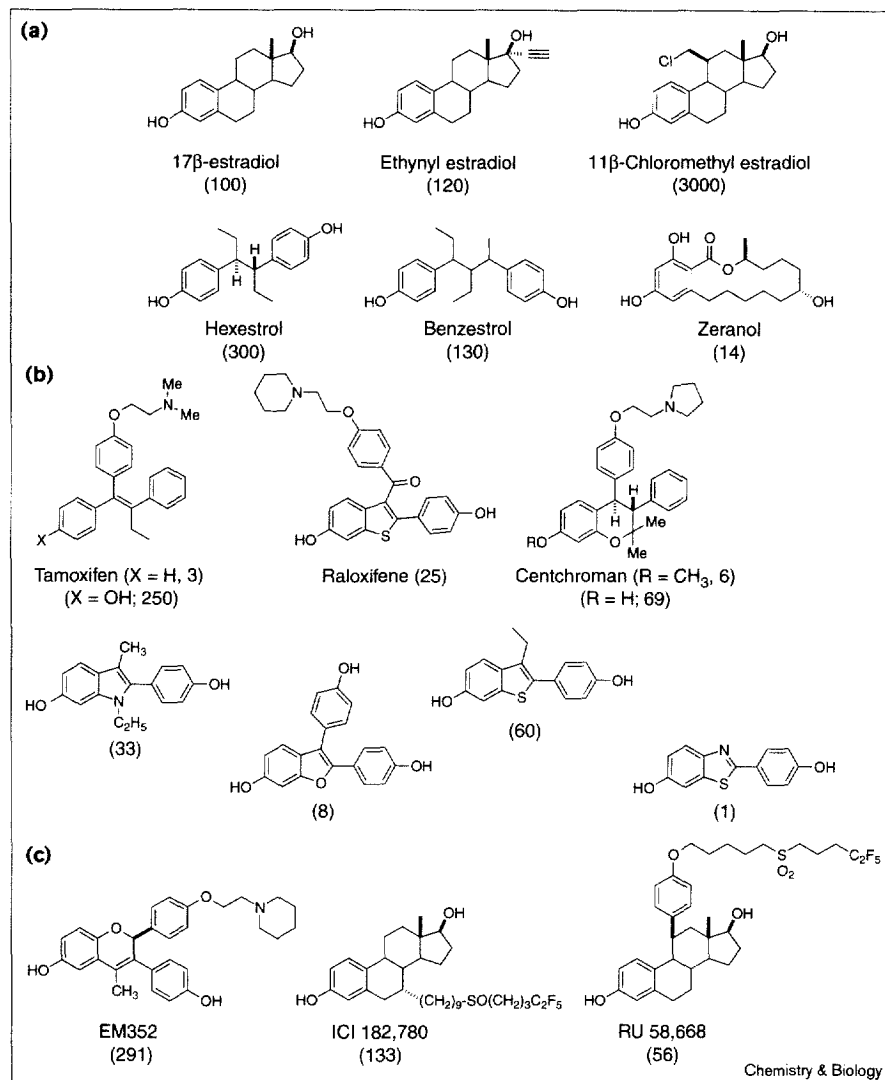
The molecular target of estrogens is the estrogen receptor (ER), of which there are now known to be two subtypes, ER- α and ER- β , that have different patterns of tissue expression and somewhat different ligand-binding specificities [2,3]. ER is a transcription factor that binds to specific estrogen-response elements in the promoter region of estrogen-regulated genes and whose activity is modulated by the estrogen ligands [4]. The capacity of ER–ligand complexes to activate gene transcription is mediated by a series of co-regulator proteins [5]. These co-regulators have interaction functions that tether ER to the RNA polymerase II preinitiation complex and enzymatic activities to modify chromatin structure [6]. It is the fact that each cell and each gene presents to an ER(subtype)–ligand complex a unique combination of these effector components—various estrogen-response elements and

co-regulators—that appears to underlie, in part, the cell and gene selectivity of various estrogens [7].

Among known ligands for ER, the natural estrogens are the simplest of the steroidal hormones, distinguished by their phenolic A-ring (Figure 1). Synthetic estrogens, especially those of nonsteroidal nature, generally retain a phenolic function (at least for those of high potency), but otherwise span a remarkable range of structural motifs that encompass simple acyclic core structures of various lengths and sizes, as well as a variety of ring-size fused and nonfused carbocyclic and heterocyclic systems [8–10]. It is clear from many decades of medicinal-chemistry investigations that minor changes in the structure and stereochemistry of these ligands can have profound effects on both their affinity and their biocharacter (i.e. the agonist versus antagonist balance in various tissues). Major efforts have been directed at optimizing ER ligand structure to obtain desired profiles of tissue selectivity, but, even so, the ideal profile for various uses has not yet been achieved [1,11,12].

As currently explored, ER ligands are, by and large, not well suited for synthesis using combinatorial approaches, because their preparation generally involves a series of carbon–carbon bond forming reactions that do not give uniformly high yields, nor are they well adapted to solid-phase-synthesis methods. There are two examples of the preparation of estrogen combinatorial libraries on solid

Figure 1



Examples of ligands with high affinity for the estrogen receptor. In each case, the binding affinity relative to that of estradiol (100%) is given in parentheses. The compounds are grouped according to their activity in a standard rat uterine weight gain assay as (a) agonists, (b) mixed or selective agonist/antagonists or (c) pure antagonists.

phase, both involving stilbene-like structures [13,14], but the application of combinatorial approaches for the preparation of ER ligands has, so far, been limited.

To expand possible combinatorial approaches to the synthesis of ER ligands, we have begun investigating simple structural motifs that might be used for the construction of molecules with high affinity for ER. The goal was to identify core structures that could be readily prepared by the types of simple condensation reactions that typify those used in solid-phase combinatorial approaches for the preparation of drug-like molecules, and from these to select ones that would support the development of high-affinity ligands for ER.

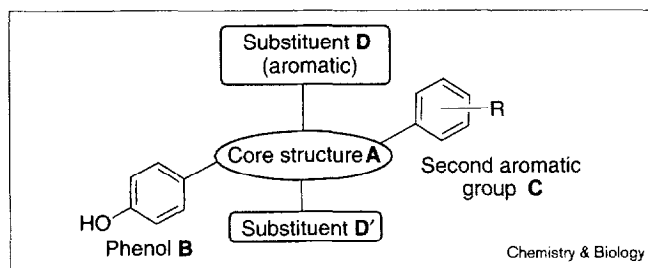
Here, we describe the investigation of prototype 1,2- and 1,3-azole systems as potential ligands for the ER. We examine the issue of whether ER ligands can be considered

simply as an assembly of a phenol unit together with 2–3 auxiliary peripheral groups linked together by a functionally inert core scaffold, or whether the core scaffold itself plays an integral role in ligand binding. In the process, we have discovered a new class of high-affinity ligands for ER, 4-alkyl-1,3,5-triarylpyrazoles, that bear an unexpected topological resemblance to the nonsteroidal estrogen raloxifene and show an interesting structure-binding affinity pattern.

Results and discussion

Structural motifs found in estrogen-receptor ligands and proposed heterocyclic surrogates

Selected examples of nonsteroidal ligands for the estrogen receptor are shown in Figure 1, together with an indication of their ER-binding affinity and their agonist (Ag) versus antagonist (Antag) character in a standard rat uterine weight gain assay. Collectively, these molecules exemplify a recognizable structural gestalt (Figure 2): a core structure (A) onto

Figure 2

Estrogen ligand pharmacophore model.

which are attached other, peripheral structural elements, a phenolic unit (B) that is always preserved, a second aromatic group (C) that is usually present, and another substituent (D) or two (D'), one of which might be aromatic. In the case of ER antagonists or mixed agonist/antagonists, one of the substituents generally contains a basic or polar function.

Comparisons of the various specific manifestations of this basic structure (Figure 1) suggest that, to achieve high

ER-binding affinity, the peripheral substituents (B–D') need to be displayed in a certain geometric arrangement, so that they will be 'in register' with their corresponding subsites in the ligand-binding pocket in ER. It seems that this peripheral group 'display function' can be accomplished by using core elements that encompass a considerable structural variety. This raises the interesting question of whether the core element itself plays any direct role in ER binding or whether it serves merely as an inert molecular scaffold whose function is simply to display these peripheral elements with appropriate topology. If the latter is true, it should be possible to replace the core scaffold with a variety of other units, providing they also are able to display the peripheral elements with the appropriate geometry. Some of these core scaffolds, namely small-ring heterocycles, could be assembled by facile condensation reactions from simpler components, a situation that is favorable for the development of large chemical libraries of related compounds by combinatorial synthesis approaches.

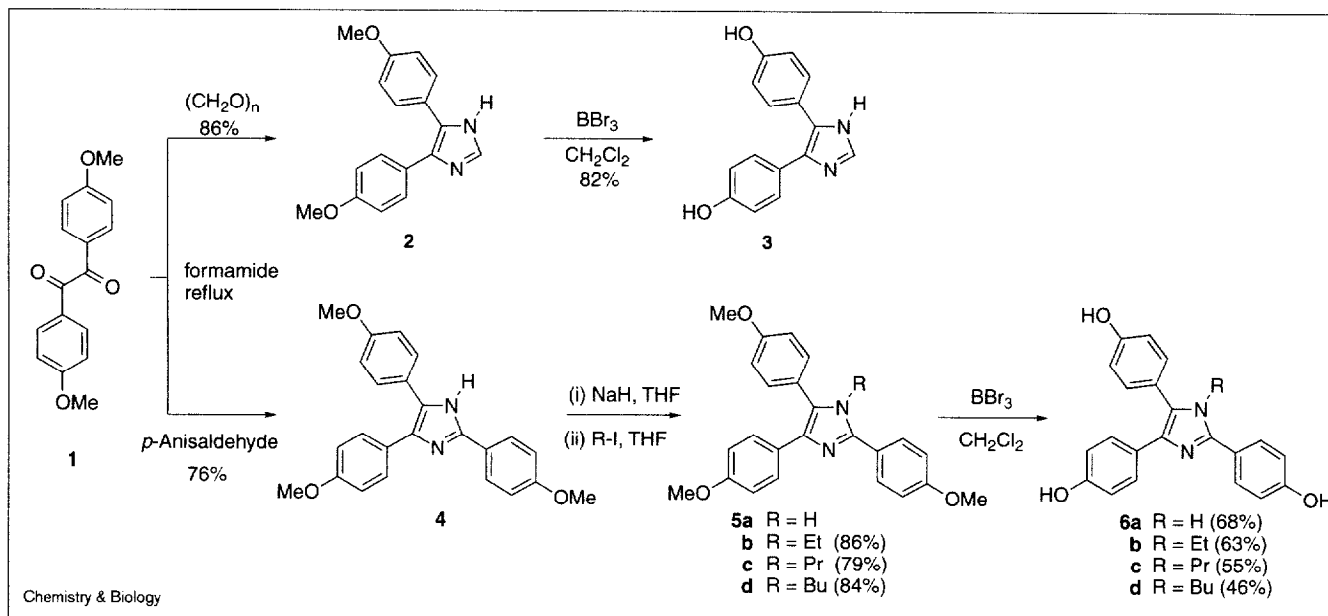
In Table 1 we have outlined two (out of many possible) manifestations of this conceptual approach, based on the incorporation of certain substructural motifs into 1,2- and

Table 1**Structural motifs found in ER ligands and proposed surrogates.**

Estrogen-receptor ligand	Structural motif	Combinatorial analog (class)
Benzestrol 	 Motif A. Homobibenzyl*	3,5-Diaryl pyrazoles
Raloxifene 	 Motif B. Bibenzyl*	3,5-Diaryl isoxazoles
Hydroxytamoxifen 	 Motif B. Bibenzyl*	2,4-Diaryl imidazoles, thiazoles, oxazoles
		4,5-Diaryl imidazoles, oxazoles, thiazoles

*These structural motifs are meant to highlight alternative atom connections between the phenol and a second aromatic substituent, without specific consideration of conformational factors. Structural motifs found in ER ligands and proposed surrogates.

Figure 3



Synthesis of imidazoles 3 and 6a-d.

1,3-azole systems. Here, the homobibenzyl motif A, exemplified in the nonsteroidal ligands benzestrol and raloxifene, is represented in various 3,5-diaryl-1,2-azoles (pyrazoles and isoxazoles) and 2,4-diaryl-1,3-azoles (imidazoles, thiazoles and oxazoles). Similarly, the bibenzyl motif B is represented in various 4,5-diaryl-1,3-azoles. In each case, the diazole N,N-systems (namely pyrazoles and imidazoles) can accommodate up to four peripheral substituents, whereas the N,O- and N,S-heterocycles (oxazoles, isoxazoles and thiazoles) are limited to three substituents.

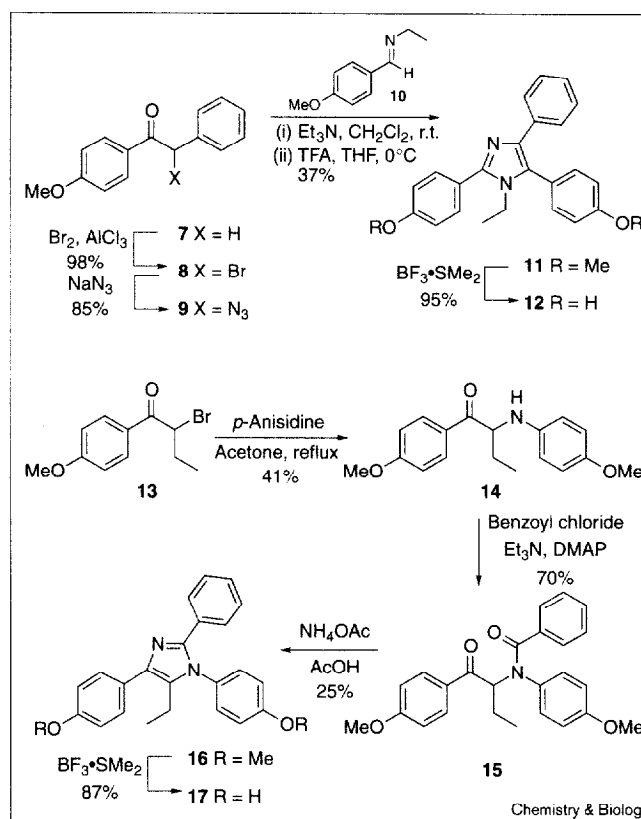
Synthesis of representative diaryl and triaryl 1,2- and 1,3-azoles as potential ligands for the estrogen receptor

Imidazoles

The synthesis of representative symmetrical members of the imidazole class and their N-alkyl analogs was accomplished by a well-precedented approach [15] shown in Figure 3. Refluxing 4,4'-dimethoxybenzil (1) in formamide in the presence of *para*-formaldehyde afforded the 4,5-disubstituted imidazole 2 [16], which upon deprotection with BBr₃ in CH₂Cl₂ afforded imidazole 3 in good yield. A similar reaction using 4-methoxybenzaldehyde afforded the 2,4,5- tri-substituted imidazole 4 [17–19] in good yield. To prepare tetra-substituted systems, the sodium salt of imidazole 4 was alkylated with ethyl, propyl and butyl iodide, and then deprotected to afford free phenols 6a–d.

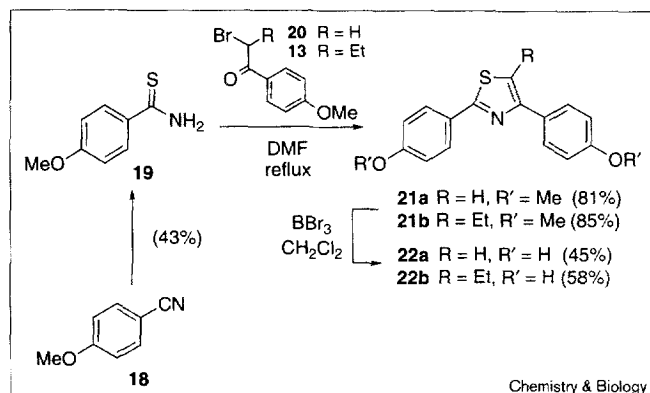
Two additional, unsymmetrical, imidazoles were synthesized as outlined in Figure 4. The top reaction sequence illustrates the synthetic approach to N-ethyl imidazole 12. Reaction of 4-methoxy-deoxybenzoin (7) [20] with bromine

Figure 4



Synthesis of imidazoles 12 and 17.

Figure 5

Synthesis of thiazoles **22a** and **22b**.

and a trace of AlCl_3 in Et_2O gave α -bromoketone **8** [21], which, upon reaction with sodium azide in acetone, afforded the corresponding azide **9**. The azido-ketone **9** was treated with one equivalent of Et_3N and imine **10** in tetrahydrofuran (THF). Removal of solvent and excess Et_3N followed by treatment of the crude intermediate 2,5-dihydro-2-hydroxyimidazole with TFA in CH_2Cl_2 , according to the procedure of Patonay and Hoffman [22], resulted in the formation of *N*-ethyl imidazole **11**. Deprotection with $\text{BF}_3 \cdot \text{SMe}_2$ in CH_2Cl_2 produced imidazole **12** in good yield.

The synthesis of *N*-aryl substituted imidazole **17** is also shown in Figure 4. Refluxing 4'-methoxy- α -bromobutyrophenone (**13**) with *p*-anisidine in acetone gave the α -amino-ketone **14**, which was converted into the benzamide **15** upon reaction with benzoyl chloride and base. Cyclization with ammonium acetate in refluxing acetic acid afforded the 1,2,4,5 tetra-substituted imidazole **16**, which upon deprotection with $\text{BF}_3 \cdot \text{SMe}_2$ in CH_2Cl_2 produced the free phenol **17**.

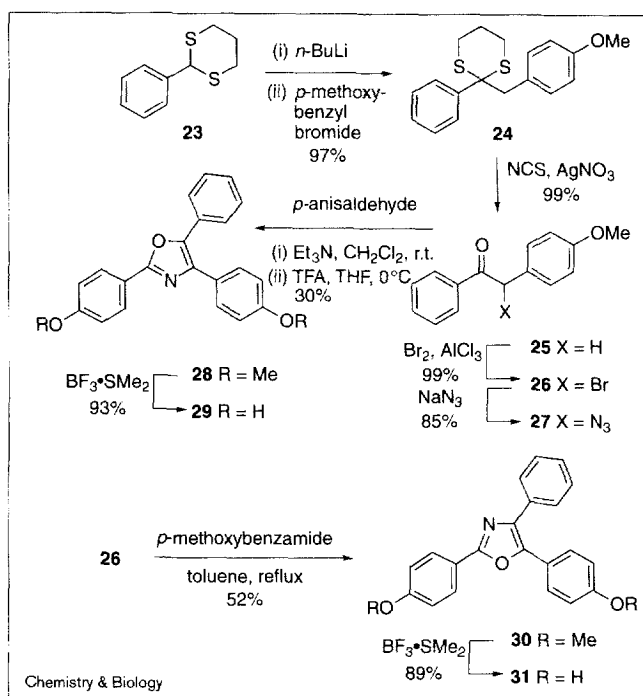
Thiazoles

The synthesis of representative thiazoles is shown in Figure 5. Thioamide **19**, derived from 4-methoxybenzonitrile (**18**) [23], was condensed with 4'-methoxy- α -bromoacetophenone (**20**) or 4'-methoxy- α -bromobutyrophenone (**13**) in refluxing DMF to give high yields of the 2,4-disubstituted thiazole **21a** [24] or 2,4,5-trisubstituted thiazole **21b**, respectively. Deprotection with BBr_3 afforded moderate yields of the free phenols **22a** and **22b**.

Oxazoles

Two representative oxazoles were synthesized as shown in Figure 6. Reaction of the lithium anion of dithiane **23** with *p*-methoxybenzyl bromide gave the alkylated product **24**, which upon hydrolysis afforded 4'-methoxy-deoxybenzoin (**25**) [25] in excellent yield. Conversion to the

Figure 6

Synthesis of oxazoles **29** and **31**.

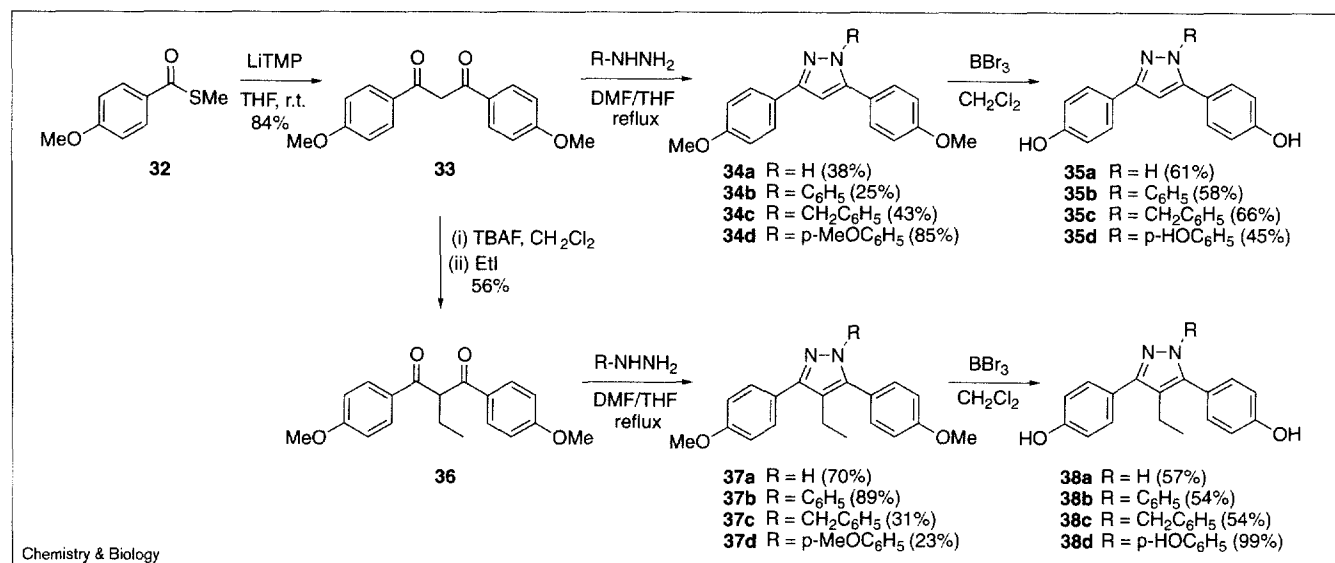
bromide **26** [26] and azide **27** was accomplished as described for analogous compounds **8** and **9** above. The azido-ketone **27** was then treated with one equivalent of Et_3N and *p*-anisaldehyde, and then with TFA to afford oxazole **28** [27]. Oxazole **30** resulted from the condensation of bromo-ketone **26** with *p*-methoxybenzamide in refluxing toluene, analogous to the thiazole synthesis discussed above. Deprotection of **28** and **30** with $\text{BF}_3 \cdot \text{SMe}_2$ gave oxazoles **29** and **31**, respectively.

Pyrazoles

The synthesis of the pyrazoles involves the condensation of a hydrazine with a 1,3-diketone [28]. Using the method of Beak and coworkers [29], we obtained 1,3-diketone **33** from the reaction of the methyl thioester **32** and lithium tetramethylpiperidide in good yield (Figure 7). Condensation of the diketone with hydrazine hydrochloride or *N*-substituted hydrazine hydrochlorides in refluxing DMF/THF (3:1) afforded the 3,5-disubstituted pyrazole **34a** or 1,3,5-trisubstituted pyrazoles **34b–d**; yields were higher with aryl-substituted hydrazines than with hydrazine itself. Deprotection of **34a–d** with BBr_3 afforded the free phenols **35a–d** in moderate yield.

The introduction of a 4-alkyl substituent was accomplished through the alkylation of diketone **33** with TBAF and ethyl iodide to afford **36** in moderate yield [30,31]. Attempts to increase the yield of this alkylation were

Figure 7

Synthesis of pyrazoles **35a-d** and **38a-d**.

unsuccessful. Conversion of diketone **36** to the corresponding pyrazoles was accomplished as with the unsubstituted case, to afford pyrazoles **38a-d**.

Isoxazoles

The preparation of a single isoxazole is shown in Figure 8 [32]. Double deprotonation of the ketoxime **39** derived from 4-methoxyacetophenone with *n*BuLi, followed by addition of methyl 4-methoxybenzoate afforded the 3,5-disubstituted isoxazole **40** in low yield [33]. Deprotection with BBr_3 afforded the free phenol **41** in moderate yield [34].

Estrogen-receptor binding

The binding affinities of the heterocycles prepared above for the estrogen receptor are shown in Tables 2-4, organized according to heterocyclic core structure. The binding values were obtained from a competitive radiometric binding assay, using $[^3\text{H}]$ estradiol as the tracer, dextran-coated charcoal

to adsorb free tracer and lamb uterine cytosol as a source of ER. The values are expressed as relative binding affinities (RBA), with estradiol having an affinity of 100% [35]. In replicate assays, these values are reproducible with a coefficient of variation of 30% (K.E. Carlson and J.A.K., unpublished observations).

Imidazoles, oxazoles and thiazoles

The receptor-binding data for the imidazole series are shown in Table 2. Although the members of this series have rather low affinity, there is an increase in RBA with the addition of alkyl substituents at the 1-position (**3**, **6a-d**); this trend reaches a maximum for propyl **6c**, reversing for the butyl substituent **6d**. Such trends, where affinity

Figure 8

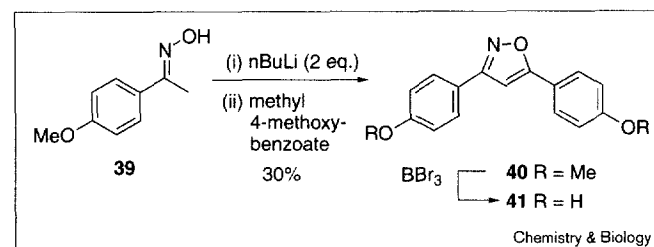
Synthesis of isoxazole **41**.

Table 2

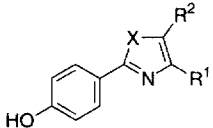
Estrogen receptor binding data for imidazoles **3**, **6a-d**, **12** and **17**.

Compound					RBA*
	R ¹	R ²	R ³	R ⁴	
3	4'-HO-C ₆ H ₄	4'-HO-C ₆ H ₄	H	H	<0.001
6a	4'-HO-C ₆ H ₄	4'-HO-C ₆ H ₄	H	4'-HO-C ₆ H ₄	0.007
6b	4'-HO-C ₆ H ₄	4'-HO-C ₆ H ₄	C ₂ H ₅	4'-HO-C ₆ H ₄	0.38
6c	4'-HO-C ₆ H ₄	4'-HO-C ₆ H ₄	C ₃ H ₇	4'-HO-C ₆ H ₄	0.62
6d	4'-HO-C ₆ H ₄	4'-HO-C ₆ H ₄	C ₄ H ₉	4'-HO-C ₆ H ₄	0.17
12	C ₆ H ₅	4'-HO-C ₆ H ₄	C ₂ H ₅	4'-HO-C ₆ H ₄	0.25
17	4'-HO-C ₆ H ₄	C ₂ H ₅	4'-HO-C ₆ H ₄	C ₆ H ₅	0.37

*RBA, relative binding affinity (estradiol = 100%).

Table 3

Estrogen receptor binding data for thiazoles **22a**, **22b** and oxazoles **29** and **31**.

				
Compound	X	R ¹	R ²	RBA
22a	S	4'-HO-C ₆ H ₄	H	0.018
22b	S	4'-HO-C ₆ H ₄	C ₂ H ₅	0.041
29	O	4'-HO-C ₆ H ₄	C ₆ H ₅	<0.001
31	O	C ₆ H ₅	4'-HO-C ₆ H ₄	0.027

increases with substituent size up to a point, are well known both in steroidal systems (11 β - and 16 α -substituents) [36] and in other non-steroidal ligand series (such as 2-phenylindoles [37], tetrahydrochrysenes [38] and so on), and probably represent the filling of preformed pockets of limited volume in the receptor by these substituents [37]. The principal difference in binding, however, is between the tetra-substituted imidazoles (**6b–d**, **12** and **17**) and the di- or tri-substituted imidazole (**3** and **6a**), the tetra-substituted ones having much higher affinity. There is little difference in binding between imidazoles **12** and **17**, which have a different arrangement of nitrogen atoms in the heterocyclic core but display their four substituents in an identical fashion (Figure 9). The overall low binding affinity of the imidazoles as a class might be the result of the high inherent polarity of this heterocyclic system as compared with the pyrazoles, reflected by their higher chromatographic polarity in both normal and reversed phases systems. It is also of note that the dipole moment for imidazole is very

Table 4

Estrogen receptor binding affinity data for pyrazoles and an isoxazole.

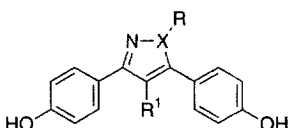
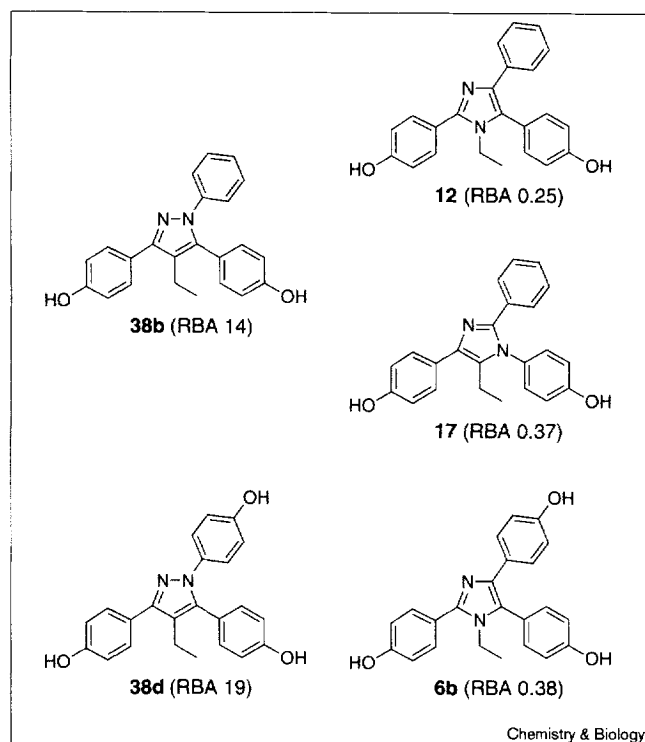
				
Compound	X	R	R ¹	RBA
35a	N	H	H	0.009
35b	N	C ₆ H ₅ -	H	0.028
35c	N	C ₆ H ₅ CH ₂ -	H	<0.007
35d	N	4'-HO-C ₆ H ₄ -	H	0.059
38a	N	H	C ₂ H ₅	0.015
38b	N	C ₆ H ₅ -	C ₂ H ₅	14.0
38c	N	C ₆ H ₅ CH ₂ -	C ₂ H ₅	0.150
38d	N	4'-HO-C ₆ H ₄ -	C ₂ H ₅	19.0
41	O	-	C ₂ H ₅	0.006

Figure 9



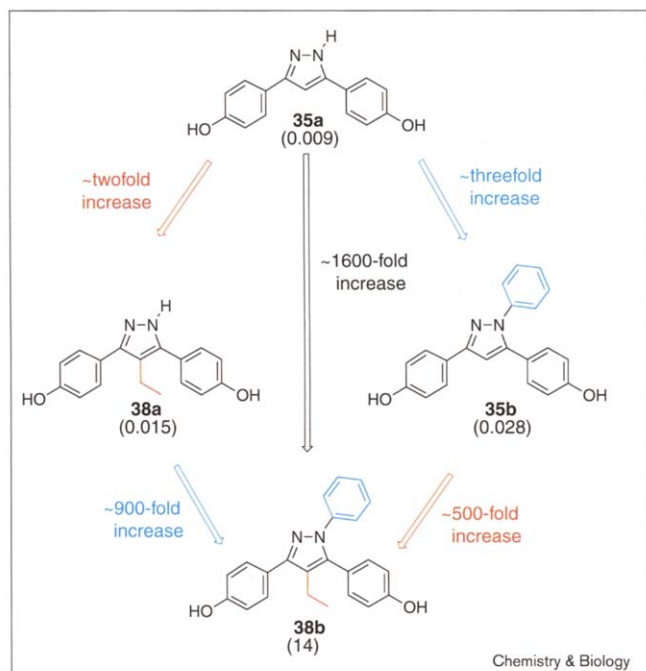
Comparisons between ring pyrazoles (**38b**, **38d**) and imidazoles (**6b**, **12** and **17**).

large, 5.56 D [39], and this might be unfavorable for binding to the estrogen receptor.

Table 3 shows the binding data for the two thiazoles and oxazoles. Although affinities are again very low, the more highly substituted thiazole again has the higher affinity (**22a** compared with **22b**). The oxazole **29** has undetectable affinity for ER. The isomer **31**, however, does have measurable, albeit low, binding. In contrast to imidazoles, thiazoles and oxazoles do not have very high dipole moments [39]; so overall polarity is not likely to be the cause of their low ER binding affinity, although heteroatom orientation appears to play a role (**29** compared with **31**). In the imidazole series, the compounds with the highest affinities were all tetra-substituted, however. As it is only possible to tri-substitute a thiazole or oxazole, this core structure might be unable to present sufficient peripheral substituents to afford ligands with good ER binding affinities, at least as far as we have investigated.

The low binding affinities of the imidazoles, thiazoles and oxazoles are disappointing, although not surprising, considering the relatively poor affinity of the most closely related benzothiazole reported by von Angerer [40] (Figure 1). The sparsely substituted monocyclic or polycyclic aromatic systems are also expected to be rather

Figure 10



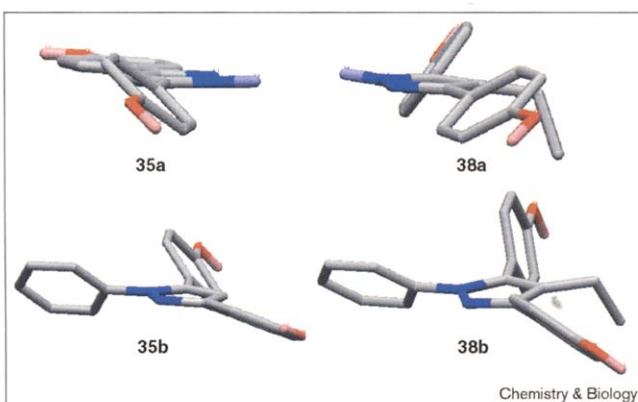
Comparison of the estrogen receptor binding affinity of four related pyrazoles with increasing substitution.

planar. It is generally agreed that good ligands for the estrogen receptor need to have some degree of 'thickness' in the central portion of the ligand [38]. When alkyl substituents are added to either the imidazoles or thiazoles, their RBA increases (Tables 2,3). This increased binding could be due to an increase in steric bulk around the central portion of the molecule, the result, in part, of a twisting of some of the aromatic substituents (see below) or to an increase in lipophilicity. Regardless, the effects are not great, and in general the 1,3-azoles seem to present some special challenges that might best be investigated further by combinatorial approaches.

Pyrazoles and isoxazoles

The RBA data for the 1,2-azoles are presented in Table 4. Immediately apparent is the relatively high binding affinity of pyrazoles **38b** and **38d**. An interesting comparison can be made among compounds **35a**, **35b**, **38a** and **38b** (Figure 10). The disubstituted progenitor **35a** has very low affinity; addition of a third substituent, 1-phenyl in **35b** or 4-ethyl in **38a**, causes only a twofold or threefold increase in binding affinity, respectively. By contrast, addition of the fourth substituent (to give **38b**) causes either an 900- or 500-fold increase in binding affinity, respectively. Clearly, this is not additive behavior—two groups that each alone raise binding affinity twofold and threefold, together raise binding not sixfold but 1600-fold. This suggests that to achieve high binding affinity there needs to be a detailed

Figure 11



Ab initio calculated conformations for **35a**, **35b**, **38a** and **38b**.

and proper match between the peripheral substituents and several subsites on the receptor, and in the azole systems we have explored, it appears that this requires a tetra-substituted ring (see below). Consistent with this is the low affinity of the isoxazole **41**, whose affinity is similar to the most closely related tri-substituted pyrazole **38a**.

There are other interesting trends in the pyrazole series: replacement of the N-phenyl substituent (**38b**) with an N-benzyl group (**38c**) causes a dramatic 100-fold reduction in binding. Both of these compounds are tetra-substituted pyrazoles, and they contain the homobibenzyl motif A that was considered to be an important factor for receptor binding (as do all of the other compounds in Table 1). The decrease in binding affinity in **38b** compared with **38c** again suggests the need for a detailed match between ligand substituents and receptor subsites: the extra 'kink' in the benzyl substituent in **38c** might be repositioning the peripheral substituents in a less favorable geometry. The addition of a hydroxyl group at the *para* position of the N-phenyl substituent (compound **38d** compared with **38b**) causes a minor increase in binding, indicating that polarity is well tolerated in this region of the receptor.

Structural comparisons between high-affinity pyrazole ligands and other nonsteroidal ligands

The conformation of pyrazoles **35a,b** and **38a,b** was determined by *ab initio* calculations at the 3-G21* level (Figure 11). The action of A-strain is evident in these structures: even in the disubstituted system **35a**, the 5-phenyl group is twisted ~60° out of the plane; this twisting increases as the third (**35b**, **38a**) and fourth (**38b**) substituents are added to the pyrazole ring, so that in **38b** the 5-phenyl substituent is nearly perpendicular to the pyrazole core. In this conformation **38b** resembles the general propeller-type conformation of the triarylethylene nonsteroidal estrogens such as tamoxifen [41].

Although the comparison of the conformations of tamoxifen with pyrazole **38b** might give some idea of the reason **38b** binds to ER with high affinity, it does not adequately explain why **35a**, **35b** and **38a** have so much lower binding affinities. When the latter three pyrazoles are compared with **38b**, it is apparent that there is little difference in conformation that could account for the large discrepancy in binding within the series. The reasons for the marked changes in RBA in response to very small changes in structure, noted especially for the pyrazole series, are therefore not intuitively obvious from an examination of the structure of the ligands alone, although they are not entirely unexpected on the basis of the behavior of other nonsteroidal ligands and the detailed fit of these congeners in the ligand-binding pocket of the estrogen receptor (see below).

Analysis of the X-ray structure of the estrogen-receptor ligand-binding domain complexed with estradiol and the nonsteroidal ligand raloxifene

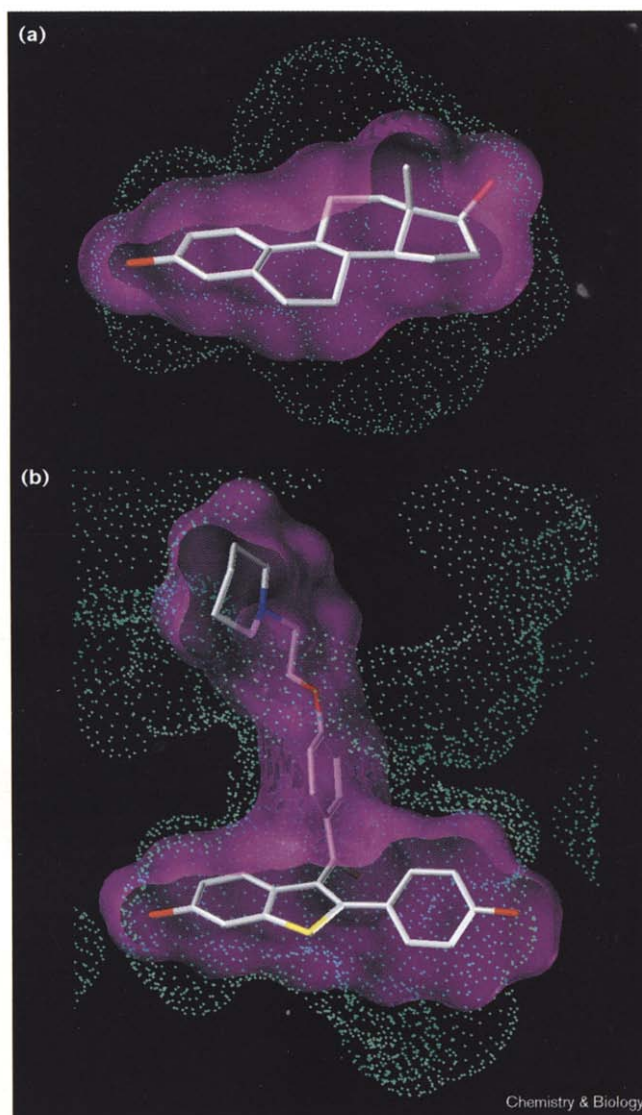
The explanation that was previously proposed — that high-affinity binding to ER derives from a proper match between the peripheral substituents on the ligand and their complementary binding regions on the receptor—can now be considered in some detail, because, recently, the X-ray structures of the estrogen receptor- α bound to estradiol and the nonsteroidal ligand raloxifene have been reported [42].

The ligand-binding pocket in the ER–estradiol structure has a volume of approximately 450 \AA^3 , which is $\sim 200 \text{ \AA}^3$ larger than the volume of estradiol [43] (Figure 12a). As a result, there is a large hydrophobic space around the central portion of the binding pocket, especially in the regions corresponding to the 11β position and, to a lesser degree, 7α position (Figure 12a), which is consistent with the tolerance that ER shows for binding steroids with large substituents at these positions [36]. A view of the ER–raloxifene structure is shown in Figure 12b. The core of this ligand is oriented in the same manner as estradiol and occupies much of the same space in the binding pocket, but the benzoyl substituent projects outward, askew of the ligand core, with the piperidinyl sidechain extending into an upper hydrophobic region, which is much more open due to the displacement of helix 12 [42].

Comparison between raloxifene and the tetra-substituted pyrazole (38b**)**

The structure of the high-affinity pyrazole (**38b**) can be overlaid onto the structure of raloxifene (Figure 13a). In such a superposition, it is evident that the centroids of all three aromatic rings lie quite close to one another. This structural alignment can be used to place the pyrazole **38b** into the ligand-binding pocket of the ER–raloxifene structure (Figure 13b). With a minimal, energetically reasonable rearrangement of nearby residues (see Figure 13 legend), this ligand can fit quite comfortably in the raloxifene pocket (compare Figure 13b with Figure 12b).

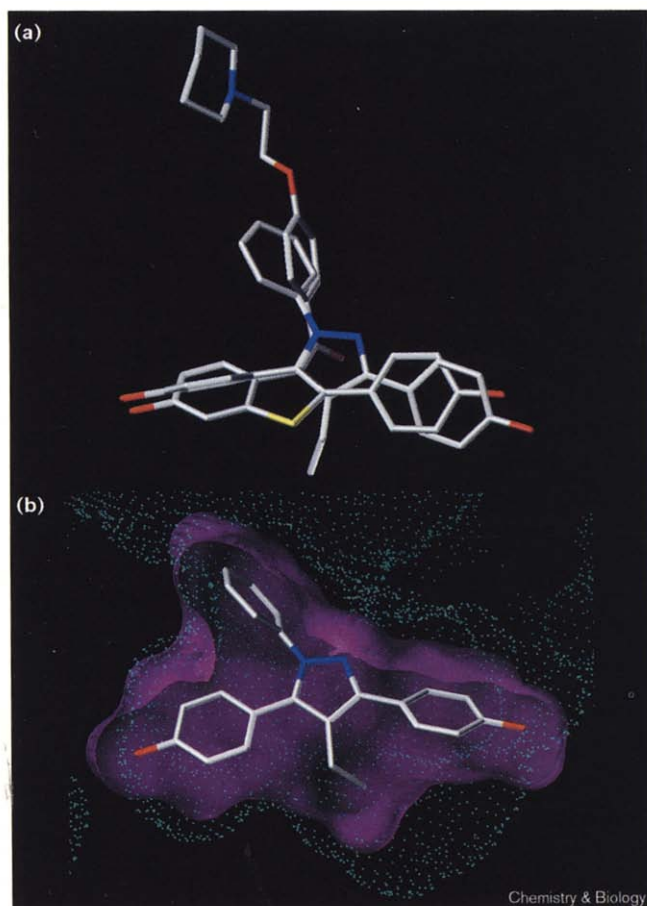
Figure 12



Ligand binding pockets for (a) estradiol and (b) raloxifene. Structures were prepared from the crystallographic coordinates [43] by generating a solvent-accessible surface for the protein (green–blue dot surface) and for the ligand (purple).

In the arrangement shown in Figure 13b, the two hydroxyl groups are positioned in such a manner that they could engage the same protein hydrogen-bonding partners as do the corresponding hydroxyl groups in raloxifene; the 3-(*p*-hydroxyphenyl) substituent of **38b** is mimicking the estradiol A-ring surrogate of raloxifene (i.e. the fused phenol of the benzothiophene unit) and the 5-(*p*-hydroxyphenyl) group of **38b** is mimicking the pendant *p*-hydroxyphenyl group at position 2 of the benzothiophene (compare with Figure 12b). The 1-phenyl group of **38b** overlies the benzoyl arene of raloxifene and projects into channel that exists in roughly the 11β direction in the ER–raloxifene

Figure 13



(a) Overlay of pyrazole **38b** with raloxifene and (b) pyrazole **38b** in the binding pocket of the ER-raloxifene structure. (a) The overlay of the two ligands was obtained by a least-squares multifitting seven atoms in each molecule ($rms=0.924$ Å): in each of the three benzene rings, the two atoms selected were the ones at the site of attachment and the ones *para* to this site; in addition, the *p*-hydroxy group on the 5-phenyl substituent in pyrazole **38b** was overlaid with the benzothiophene hydroxyl group. (b) Pyrazole **38b** was pre-positioned into the ER-raloxifene crystal structure [42] from the overlay shown in (a). From this structure additional docking studies using FlexiDock (Tripos, St Louis, MO) followed by a three-step minimization using the TRIPOS Forcefield were conducted to afford the final model (see the Materials and methods section). This minimization caused only small changes in the protein and ligand, but reduced the ligand-protein interaction energy to a reasonable level.

structure. The 4-ethyl substituent on pyrazole **38b** projects outwards from the heterocycle from a position that corresponds roughly to the sulfur atom of the benzothiophene ring system, and extends into an open pocket in the ER.

When analyzed in this manner, one can appreciate that the pyrazole core can display these four substituents in a manner congruent with the same regions in the binding pocket of the estrogen receptor that accommodate corresponding portions of raloxifene. In addition, the high cost in binding affinity that results from the absence of

either the 1-phenyl or the 4-ethyl substituent (compare with Figure 10) suggests that proper registration of each of the four peripheral substituents into its appropriate binding subsite is supported by the interaction of the other three. By this analysis, it is therefore not surprising that all of the other heterocyclic systems that were only di-substituted or tri-substituted were low affinity ligands, at least with the substituents we have thus far investigated. The low-affinity of the tetra-substituted imidazoles, however, most likely derives from their high polarity, as noted (see below).

The importance of core structural element in ligand binding: passive or active?

The question raised initially—does the core scaffold in these novel ER ligands play only a passive role in their binding, merely displaying the peripheral substituents in an appropriate topology, or is its role more active or functional?—can be answered reasonably definitively from the results we have obtained so far. Clearly, with the substituents we have examined, high-affinity binding was obtained only with those azoles that afforded the possibility of tetra-substitution. But of these, the 1,2-diazoles (pyrazoles) and the 1,3-diazoles (imidazoles), only the pyrazoles gave good binding. Although there are not many direct comparisons that can be made between these two diazole systems, pyrazole **38b** and imidazoles **12** and **17** are, in fact, just ring nitrogen isomers of one another, having otherwise identical peripheral groups and functionality (Figure 9). The same is true for pyrazole **38d** and imidazole **6b**. In both cases, however, the pyrazole partner binds to ER with ~30–36-fold higher affinity than the isomeric imidazole(s). This would suggest that the core structure does play more than a passive role in ER binding, although, as noted before, the high polarity and significant dipole moment of the imidazole might be the principal reason for the difference in this case. The issue of the functional role of the core scaffold in ER binding needs to be investigated further in these and other heterocyclic systems.

Significance

Compounds with a remarkable variety of structures bind with high affinity to the estrogen receptor (ER), and many nonsteroidal ligands have been prepared in the search for agents that have improved tissue-selectivity profiles. The application of combinatorial approaches to the development of selective ER ligands, however, is still in a state of infancy.

Based on a simple pharmacophore model consisting of a core scaffold and various peripheral groups we have designed systems that display the peripheral groups on simple heterocyclic core systems, which are readily prepared by simple condensation reactions. Here, we describe the synthesis and ER-binding affinity of various substituted 1,2- and 1,3-azoles.

No significant binding was found for members of the imidazole, thiazole or isoxazole classes, and this is rationalized either by the inherent polarity of these compounds (imidazoles) or by their inability to carry a sufficient number of the types of peripheral substituents we have explored so far (thiazoles, oxazoles and isoxazoles). Several members of the pyrazole class did show good binding affinity, however, the best being a tetra-substituted pyrazole **38d**. Both **38b** and **38d** bear an unexpectedly close conformational relationship to the nonsteroidal ligand raloxifene.

Compounds such as **38b** and **38d** are well suited to combinatorial synthesis using solid-phase methods. The large differences in binding affinity that result from small structural changes suggest that a thorough investigation of many possible combinations of core structures and peripheral substituents will be needed to identify novel high-affinity ligands for the ER that can be evaluated for their selective biological activity. The solid-phase combinatorial synthesis of pyrazole libraries is currently underway and has yielded other high-affinity ligands for the estrogen receptor (S.R.S. and J.A.K., unpublished observations). Some of these heterocycles have also shown intriguing biological activity [43].

Materials and methods

General methods

All reactions using water- or air-sensitive reagents were conducted under an Ar atmosphere with dry solvents. Solvents were distilled under N₂ as follows: CH₂Cl₂ from CaH₂, tetrahydrofuran (THF) from sodium benzophenone ketyl, dimethylformamide (DMF) from MgSO₄, and hexanes from CaSO₄. Triethylamine was distilled over CaH₂. All other reagents were purchased from commercial suppliers and used without further purification. Reactions were all monitored using thin-layer chromatography (TLC), performed on 0.25 mm silica gel glass plates containing F-254 indicator. Visualization on TLC was achieved by UV light (254 nm), iodine vapors, or phosphomolybdic acid indicator. Flash chromatography was performed using Woelm 32–63 µm silica gel packing unless otherwise noted.

¹H NMR and ¹³C NMR spectra were recorded on a Varian U400, Varian U500 or Varian INOVA 750. NMR spectra chemical shifts (δ) are reported in parts per million downfield from TMS and referenced with either TMS internal standard for CDCl₃, acetone-*d*₆, MeOD-*d*₄, or DMSO-*d*₆ solvent peak. NMR coupling constants are reported in Hertz. Electron ionization (EI) spectra were obtained using a Finnigan–MATCH5 spectrometer at 70 eV. Fast atom bombardment (FAB) were recorded on a VG ZAB-SE spectrometer. High-pressure liquid chromatography (HPLC) was performed on a SpectraPhysics P100 solvent delivery system with ultraviolet detection at 254 nm. Elemental analysis was performed by the Microanalytical Service Laboratory at the University of Illinois. All characterized compounds are chromatographically homogeneous.

Relative binding affinities

Assays were performed as reported previously [44] using lamb uterine cytosol diluted to approximately 1.5 nM of receptor, which was incubated with buffer of several concentrations of unlabeled competitor together with 10 nM [³H]estradiol for 18–24 h. Free ligand was removed by adsorption onto dextran-coated charcoal. Unlabeled competitors were prepared in 1:1 DMF:TEA to ensure solubility.

Molecular modeling and docking studies

Solvent-accessible surfaces were generated (Figures 12 and 13) using the QCPE Connolly Program module (Indiana University) in Sybyl 6.5 (Tripos, St. Louis, MO). Figure 13b: the pre-positioned pyrazole **38b** was used for additional docking studies using the Tripos FlexiDock module. Both hydrogen-bond donors and acceptors within the pocket surrounding the ligand and the ligand itself in addition to select rotatable torsional bonds were defined in order to afford an optimal docked-structure prior to molecular mechanics minimization. With the protein backbone held rigid, the ligand and the protein residues within 8 Å of the ligand were then minimized using a step-wise approach: first torsional bonds about the ligand were minimized holding the receptor fixed, followed by minimization of the receptor holding the ligand fixed, and then minimization of both the ligand and receptor. Minimizations were done using the TRIPOS Forcefield (as implemented in the program Sybyl) with the Powell gradient method and default settings (final RMS < 0.05 kcal/mol-Å).

Representative chemical synthesis

4,5-Di(4-methoxyphenyl)-1H-imidazole (2). To 4,4'-dimethoxybenzil (**1**) (2.0 g, 7.4 mmol) and *p*-formaldehyde (1.0 g, 11.1 mmol) was added formamide (50 ml). The bright yellow suspension was heated to reflux (220°C) for 2 h. The reaction mixture was then cooled to room temperature then to 0°C. The crystals that formed were filtered and recrystallized from EtOAc to afford **2** (2.4 g, 86%). mp 183–184°C [lit [16] mp 183–184°C]; ¹H NMR (400 MHz, MeOH-*d*₄) δ 7.64 (s, 1H), 7.44 (d, 4H, *J* = 7.50), 6.89 (d, 4H, *J* = 7.50), 3.79 (s, 6H); ¹³C NMR (100 MHz, MeOH-*d*₄) δ 158.4, 135.2, 129.1, 128.9, 122.6, 114.2, 55.3.

General demethylation procedure using BBr₃. To a stirring solution of the methyl-protected heterocycle (1 equiv) in CH₂Cl₂ at –78°C was added a solution of BBr₃ (4–5 equiv) as a 1N solution in CH₂Cl₂. The reaction were allowed to warm to room temperature and stirred for 18 h. After quenching with H₂O, the layers were separated and the aqueous layer extracted with EtOAc (3 × 5 ml). The combined organic layers were dried over Na₂SO₄, filtered and concentrated to afford the crude phenols. Flash chromatography afforded the demethylated products.

4,5-Di(4-hydroxyphenyl)-1H-imidazole (3). Imidazole **2** (100 mg, 0.35 mmol) afforded **3** (52 mg, 59%) by the general BBr₃ demethylation procedure. ¹H NMR (400 MHz, CDCl₃) δ 14.56 (br s, 1H), 9.93 (br s, 1H), 9.24 (s, 1H), 7.24 (d, 4H, *J* = 8.47), 6.82 (d, 4H, *J* = 8.40); MS (FAB) *m/z* (relative intensity, %) 253.1 (MH⁺ 24), 169.2 (100).

2,4,5-Tri(4-methoxyphenyl)-1H-imidazole (4). A suspension of 4,4'-dimethoxybenzil (**1**) (4.0 g, 15 mmol) and *p*-anisaldehyde (20 ml, 164 mmol) and formamide (100 ml) was heated to reflux (220°C) for 2 h, during which time the reaction mixture became homogeneous. The reaction was then cooled to 0°C and the precipitated product **4** was filtered. The light yellow powder was recrystallized from MeOH/H₂O to afford 3.80 g of **4** [19] (66%). mp 89–91°C [lit [19] mp 88–94°C]. ¹H NMR (400 MHz, Acetone-*d*₆) δ 7.98 (d, 2H, *J* = 8.88), 7.42 (d, 4H, *J* = 8.52), 7.01 (d, 2H, *J* = 8.83), 6.92 (br s, 4H), 3.79 (s, 3H), 3.75 (s, 6H); ¹³C NMR (100 MHz, Acetone-*d*₆) δ 162.4, 159.9, 158.9, 145.4, 131.0, 129.0, 128.9, 126.6, 132.8, 114.0, 113.7, 113.6; MS (EI, 70 eV) *m/z* (relative intensity, %) 386.2 (M⁺, 100), 371 (30), 280 (100), 265 (30); HRMS calc'd for C₂₁H₁₆N₂O₃: 345.123800, found: 345.123918.

General N-alkylation procedure for imidazoles. A solution of imidazole **4** (200 mg, 0.52 mmol) in THF (10 ml) and DMF (1.5 ml) was cooled to 5°C. NaH (31 mg, 0.78 mmol) was added as 60% dispersion in mineral oil. The reaction mixture was warmed to room temperature for 1 h and respective alkyl halide (0.04 ml, 0.62 mmol) was added. The resulting suspension was heated to reflux for 12 h, then cooled to room temperature. The light precipitate was filtered, and the filtrate was concentrated under vacuum to a yellow solid which was flashed on silica (30% EtOAc/Hexanes) to afford alkylated products **5b–d** in 80–90% yields.

1-Ethyl-2,4,5-tri(4-methoxyphenyl)-imidazole (5b). ¹H NMR (400 MHz, CDCl₃) δ 7.60 (AA'XX', 2H, *J*_{AX} = 8.88, *J*_{AA} = 2.51), 7.46 (AA'XX', 2H,

$J_{AX} = 8.97$, $J_{AA} = 2.56$), 7.32 (AA'XX', 2H, $J_{AX} = 8.88$, $J_{AA} = 2.56$), 7.00 (AA'XX', 2H, $J_{AX} = 8.88$, $J_{AA} = 2.51$), 6.99 (AA'XX', 2H, $J_{AX} = 8.88$, $J_{AA} = 2.56$), 6.74 (AA'XX', 2H, $J_{AX} = 8.97$, $J_{AA} = 2.56$), 3.87 (q, 2H, $J = 7.32$), 3.87 (s, 3H), 3.85 (s, 3H), 1.00 (t, 3H, $J = 7.14$); ^{13}C NMR (100 MHz, CDCl_3) δ 160.0, 159.7, 158.1, 146.8, 137.2, 132.4, 130.5, 127.9, 127.5, 123.8, 123.7, 114.5, 114.0, 113.5, 55.3, 55.2, 55.1, 39.5, 16.2.

2,4,5-Tri(4-hydroxyphenyl)-1H-imidazole (6a). According to the general BBR_3 demethylation procedure above, imidazole **4** (3.0 g, 7.8 mmol) afforded **6a** as a green-orange solid that darkened upon exposure to air (1.8 g, 68%). mp 203–205°C; ^1H NMR (400 MHz, Acetone- d_6) δ 7.93 (AA'XX', 2H, $J_{AX} = 8.97$, $J_{AA} = 2.47$), 7.40 (AA'XX', 4H, $J_{AX} = 8.60$, $J_{AA} = 2.47$), 6.89 (AA'XX', 2H, $J_{AX} = 8.97$, $J_{AA} = 2.47$), 6.80 (AA'XX', 2H, $J_{AX} = 8.60$, $J_{AA} = 2.47$); ^{13}C NMR (100 MHz, Acetone- d_6) δ 157.9, 156.4, 145.9, 129.0, 126.8, 124.0, 123.4, 121.3, 115.0, 114.7; MS (FAB) m/z (relative intensity, %) 345.1 ($\text{M}+\text{H}^+$, 10), 353 (10), 169 (100); HRMS calc'd for $\text{C}_{21}\text{H}_{16}\text{N}_2\text{O}_3$: 345.123800, found: 345.123918.

1-Ethyl-2,4,5-tri(4-hydroxyphenyl)-imidazole (6b). According to the general BBR_3 demethylation procedure above, imidazole **5b** (185 mg, 0.46 mmol) afforded **6b** (107 mg, 62%). mp 150–153°C; ^1H NMR (400 MHz, Acetone- d_6) δ 7.51 (AA'XX', 2H, $J_{AX} = 8.52$, $J_{AA} = 2.42$), 7.34 (AA'XX', 2H, $J_{AX} = 8.71$, $J_{AA} = 2.39$), 7.24 (AA'XX', 2H, $J_{AX} = 8.63$, $J_{AA} = 2.41$), 6.97 (AA'XX', 2H, $J_{AX} = 8.58$, $J_{AA} = 2.31$), 6.90 (AA'XX', 2H, $J_{AX} = 8.75$, $J_{AA} = 2.31$), 6.64 (AA'XX', 2H, $J_{AX} = 8.96$, $J_{AA} = 2.43$), 3.93 (q, 2H, $J = 7.19$), 0.98 (t, 3H, $J = 7.12$); ^{13}C NMR (100 MHz, Acetone- d_6) δ 158.2, 157.9, 155.9, 146.5, 136.8, 132.5, 130.3, 127.9, 127.8, 126.6, 122.5, 122.4, 116.0, 115.4, 114.8, 17.9, 15.4; MS (FAB) m/z (relative intensity, %) 372.1 ($\text{M}+\text{H}^+$, 100), 343 (15), 275 (10), 214 (25), 162 (30), 148 (30); HRMS calc'd for $\text{C}_{23}\text{H}_{20}\text{N}_2\text{O}_3$: 372.147251, found: 372.147393.

1-Ethyl-2,5-(4-methoxyphenyl)-4-phenyl imidazole (11). Azido-ketone **9** (50.0 mg, 0.187 mmol) and imine **10** (92.0 mg, 0.564 mmol) were dissolved in THF (15 ml). Et_3N (29.0 μL , 0.208 mmol) was added via syringe and reaction stirred at room temperature for 48 h. The reaction mixture was then poured into H_2O and extracted with CH_2Cl_2 , organic fractions were pooled, dried over Na_2SO_4 , filtered and solvent removed under reduced pressure. The intermediate, 2,5-dihydro-2-hydroxyimidazole, used in next step without further purification or characterization, was taken up CH_2Cl_2 (10 ml). Solution was cooled to 0°C and TFA (14.4 μL , 0.187 mmol) was added via syringe. Reaction stirred at 0°C for 36 h. The mixture was diluted with CH_2Cl_2 (10 ml) and washed with H_2O , sat. NaHCO_3 , and sat. NaCl successively. The organic fraction was dried over Na_2SO_4 , filtered and solvent removed under reduced pressure. Purification by flash column chromatography (1:2 EtOAc:Hexanes) and recrystallization from CH_2Cl_2 /Hexanes afforded imidazole **11** as a white solid (24.6 mg, 34% yield from azide **9**). ^1H NMR (500 MHz, CDCl_3) δ 7.63 (AA'XX', 2H, $J_{AX} = 8.81$, $J_{XX'} = 2.53$), 7.54 (m, 2H), 7.34 (AA'XX', 2H, $J_{AX} = 8.80$, $J_{XX'} = 2.45$), 7.20 (m, 2H), 7.12 (m, 1H), 7.02 (AA'XX', 2H, $J_{AX} = 8.78$, $J_{AA'} = 2.54$), 7.01 (AA'XX', 2H, $J_{AX} = 8.43$, $J_{AA'} = 2.57$), 3.90 (q, 2H, $J = 7.08$), 3.89 (s, 3H), 3.87 (s, 3H), 1.02 (t, 3H, $J = 7.17$); ^{13}C NMR (125 MHz, CDCl_3) δ 200.8, 160.0, 159.8, 147.0, 134.8, 132.3 (2), 130.5 (2), 129.3, 128.9, 128.0 (2), 126.6 (2), 126.0, 123.6, 114.5 (2), 114.0 (2), 55.33, 55.28, 36.4, 16.2; MS (EI, 70 eV) m/z 384.2 (M^+); Anal. calc'd for $\text{C}_{25}\text{H}_{24}\text{N}_2\text{O}_2$: C: 78.10%, H: 6.29%, N: 7.29%, found, C: 77.91%, H: 6.28%, N: 7.28%.

General demethylation procedure using $\text{BF}_3 \cdot \text{SMe}_2$. To a stirring solution of the methyl protected heterocycle (1 equiv) in CH_2Cl_2 (8 ml) at room temperature was added $\text{BF}_3 \cdot \text{SMe}_2$ complex (75 equiv). After stirring for 24 h, solvent and excess reagent were evaporated under nitrogen stream in hood. Residue was taken up in EtOAc and washed with H_2O and sat. NaCl . Organic extract was dried over Na_2SO_4 , filtered and solvent removed under reduced pressure. The resulting residue was purified through a silica plug, eluting with EtOAc. Solvent evaporation afforded the deprotected products.

1-Ethyl-2,5-(4-hydroxyphenyl)-4-phenyl imidazole (12). Imidazole **11** (12.0 mg, 0.031 mmol) was demethylated according to the general $\text{BF}_3 \cdot \text{SMe}_2$ procedure to afford imidazole **12** as an off-white powder (10.6 mg, 95%). ^1H NMR (500 MHz, Acetone- d_6) δ 7.80 (AA'XX', 2H, $J_{AX} = 8.81$, $J_{XX'} = 2.44$), 7.47–7.49 (m, 2H), 7.44 (AA'XX', 2H, $J_{AX} = 8.65$, $J_{XX'} = 2.44$), 7.37–7.40 (m, 3H), 7.14 (AA'XX', 2H, $J_{AX} = 8.80$, $J_{AA'} = 2.43$), 7.06 (AA'XX', 2H, $J_{AX} = 8.68$, $J_{AA'} = 2.46$), 4.25 (q, 2H, $J = 7.28$), 1.17 (t, 3H, $J = 7.29$); MS (FAB) m/z 357.2 ($\text{M}+\text{H}^+$); HRMS calc'd for $\text{C}_{23}\text{H}_{21}\text{N}_2\text{O}_2$: 357.160303, found: 357.160000.

5-Ethyl-1,4-(4-methoxyphenyl)-2-phenyl imidazole (16). Keto-amide **15** (110.0 mg, 0.273 mmol) and ammonium acetate (105.0 mg, 1.362 mmol) were heated to reflux in acetic acid (10 ml) for 48 h. Acetic acid was removed under reduced pressure, resulting residue was taken up in EtOAc, washed with sat. NaHCO_3 , H_2O , and sat. NaCl . Organic extracts were dried over Na_2SO_4 , filtered and solvent removed. Product was purified by flash column chromatography (1:4 EtOAc:Hexanes) and recrystallization from CH_2Cl_2 /Hexanes to give imidazole **16** as a white solid (25.7 mg, 25%). ^1H NMR (500 MHz, CDCl_3) δ 7.72 (AA'XX', 2H, $J_{AX} = 8.29$, $J_{XX'} = 2.55$), 7.14 (m, 2H), 7.21 (m, 3H), 7.19 (AA'XX', 2H, $J_{AX} = 9.33$, $J_{XX'} = 2.71$), 6.98 (AA'XX', 2H, $J_{AX} = 8.48$, $J_{AA'} = 2.52$), 6.96 (AA'XX', 2H, $J_{AX} = 8.62$, $J_{AA'} = 2.74$), 3.87 (s, 3H), 3.85 (s, 3H), 2.67 (q, 2H, $J = 7.48$), 1.01 (t, 3H, $J = 7.45$); MS (EI, 70 eV) m/z 384.2 (M^+).

5-Ethyl-1,4-(4-hydroxyphenyl)-2-phenyl imidazole (17). Imidazole **16** (25.0 mg, 0.065 mmol) was demethylated as outlined in general $\text{BF}_3 \cdot \text{SMe}_2$ procedure above to give deprotected imidazole **17** as an off-white powder (20.2 mg, 87%). ^1H NMR (400 MHz, Acetone- d_6) δ 9.04 (br s, 1H), 8.51 (br s, 1H), 7.64 (AA'XX', 2H, $J_{AX} = 8.73$, $J_{XX'} = 2.51$), 7.50–7.47 (m, 2H), 7.31–7.27 (m, 5H), 7.01 (AA'XX', 2H, $J_{AX} = 8.94$, $J_{AA'} = 2.76$), 6.94 (AA'XX', 2H, $J_{AX} = 8.73$, $J_{AA'} = 2.52$), 2.69 (q, 2H, $J = 7.48$), 1.02 (t, 3H, $J = 7.49$); MS (FAB) m/z 357.1 ($\text{M}+\text{H}^+$); HRMS calc'd for $\text{C}_{23}\text{H}_{21}\text{N}_2\text{O}_2$: 357.1603, found 357.1602.

2,4-Di(4-methoxyphenyl)-thiazole (21a). A suspension of thioamide **19** (1.3 g, 7.9 mmol) and α -bromo-4'-methoxy-acetophenone (**20**) (1.8 g, 7.9 mmol) in DMF (10 ml) was heated to reflux for 1 h, until it became homogeneous. The heat was removed and the reaction was stirred for 15 h at room temperature. The reaction mixture was poured into H_2O (50 ml) and the solid precipitate was filtered to afford crude **21a**. Recrystallization from CH_3NO_2 afforded pure **21a** as light yellow crystals (1.8 g, 81%). ^1H NMR (400 MHz, CDCl_3) δ 7.98 (AA'XX', 2H, $J_{AX} = 8.87$, $J_{AA} = 2.53$), 7.63 (AA'XX', 2H, $J_{AX} = 8.94$, $J_{AA} = 2.48$), 6.86 (AA'XX', 2H, $J_{AX} = 8.87$, $J_{AA} = 2.53$), 6.85 (AA'XX', 2H, $J_{AX} = 8.94$, $J_{AA} = 2.48$), 7.26 (s, 1H), 3.86 (s, 3H), 3.85 (s, 3H); ^{13}C NMR (400 MHz, CDCl_3) δ 167.5, 160.9, 159.4, 155.6, 127.9, 127.6, 127.4, 126.6, 114.1, 113.9, 109.9, 55.3, 55.2; MS (EI, 70 eV) m/z (relative intensity, %) 297.1 (M^+ , 100), 282.1 (10), 164.1 (30), 149.1 (55), 133.1 (10), 121.1 (25), 77.1 (15); HRMS calc'd for $\text{C}_{17}\text{H}_{15}\text{N}_2\text{SO}_2$: 297.082469, found: 297.082351.

2,4-Di(4-hydroxyphenyl)-thiazole (22a). Thiazole **21a** (1.0 g, 3.6 mmol) was demethylated using BBR_3 as outlined in the general procedure above to afford **22a** (430 mg, 45%). mp 218–221°C; ^1H NMR (400 MHz, Acetone- d_6) δ 8.84 (br s, 2H), 7.92 (AA'XX', 4H, $J_{AX} = 8.57$, $J_{AA} = 2.17$), 7.58 (s, 1H), 6.96 (AA'XX', 2H, $J_{AX} = 8.79$, $J_{AA} = 2.51$), 6.92 (AA'XX', 2H, $J_{AX} = 8.78$, $J_{AA} = 2.44$); ^{13}C NMR (100 MHz, Acetone- d_6) δ 168.2, 159.3, 157.2, 155.8, 127.7, 127.3, 126.2, 125.1, 115.2, 114.9, 109.3; MS (EI, 70 eV) m/z (relative intensity, %) 296.1 (M^+ , 100), 150.1 (27), 121.1 (11), 78.1 (8); HRMS calc'd for $\text{C}_{15}\text{H}_{11}\text{N}_2\text{SO}_2$: 269.051163, found: 269.051051.

2,4-(4-Methoxyphenyl)-5-phenyl oxazole (28). Azido-ketone **27** (0.18 g, 0.673 mmol) and *p*-anisaldehyde (0.25 ml, 2.05 mmol) were dissolved in THF (15 ml). Et_3N (94.0 μL , 0.674 mmol) was added via syringe and reaction stirred at room temperature for 48 h. The reaction mixture was then poured into H_2O and extracted with CH_2Cl_2 , organic fraction was dried over Na_2SO_4 , filtered and solvent removed under reduced pressure. Resulting intermediate 2,5-dihydro-5-hydroxyoxazole, used in next

step without further purification or characterization, was taken up CH_2Cl_2 (10 ml). Solution was cooled to 0°C and TFA (54.0 μl , 0.701 mmol) was added via syringe. Reaction stirred at 0°C for 36 h. The mixture was diluted with CH_2Cl_2 (10 ml) and washed with H_2O , sat. NaHCO_3 , and sat. NaCl successively. Organic extracts were combined, dried over Na_2SO_4 , filtered and solvent removed under reduced pressure. Purification by flash column chromatography (1:2 EtOAc:hexanes) and recrystallization from CH_2Cl_2 /Hexanes afforded oxazole **28** as a white solid (72.4 mg, 30% yield from azide **27**). mp 125–128 $^\circ\text{C}$ (lit. [27] mp 126–127 $^\circ\text{C}$); ^1H NMR (500 MHz, CDCl_3) δ 7.84 (AA'XX', 2H, $J_{\text{AX}}=8.89$, $J_{\text{XX'}}=2.47$), 7.43 (AA'XX', 2H, $J_{\text{AX}}=8.83$, $J_{\text{XX'}}=2.48$), 7.53 (m, 2H), 7.32 (m, 2H), 7.26 (tt, 1H, $J=7.03$, 1.42), 6.97 (AA'XX', 2H, $J_{\text{AX}}=8.85$, $J_{\text{AA'}}=2.53$), 6.88 (AA'XX', 2H, $J_{\text{AX}}=8.70$, $J_{\text{AA'}}=2.53$), 3.84 (s, 3H), 3.81 (s, 3H).

2,4-(4-Hydroxyphenyl)-5-phenyl oxazole (29). Oxazole **28** (22.0 mg, 0.062 mmol) was demethylated according to the general $\text{BF}_3\cdot\text{SMe}_2$ procedure above to give deprotected oxazole **29** as an off-white powder (18.8 mg, 93%). ^1H NMR (500 MHz, Acetone- d_6) δ 9.43 (br s, 1H), 8.90 (br s, 1H), 8.08 (AA'XX', 2H, $J_{\text{AX}}=9.06$, $J_{\text{XX'}}=2.62$), 7.61 (m, 2H), 7.49 (m, 3H), 7.44 (AA'XX', 2H, $J_{\text{AX}}=8.97$, $J_{\text{XX'}}=2.44$), 7.12 (AA'XX', 2H, $J_{\text{AX}}=8.87$, $J_{\text{AA'}}=2.50$), 6.95 (AA'XX', 2H, $J_{\text{AX}}=8.86$, $J_{\text{AA'}}=2.42$); MS m/z 329.1 (M^+); HRMS calc'd. for $\text{C}_{21}\text{H}_{15}\text{NO}_3$: 329.1052, found 329.1285.

2,5-(4-Methoxyphenyl)-4-phenyl oxazole (30). A solution of bromo-ketone **26** (87.0 mg, 0.285 mmol) and *p*-methoxybenzamide (43.0 mg, 0.285 mmol) in toluene was heated to reflux for 36 h. Toluene was removed under reduced pressure and resulting residue purified by flash column chromatography (1:4 EtOAc:Hexanes). Recrystallization of desired product from CH_2Cl_2 /hexanes afforded oxazole **30** as a colorless solid (52.9 mg, 52%). mp 147–149 $^\circ\text{C}$; ^1H NMR (500 MHz, CDCl_3) δ 8.08 (AA'XX', 2H, $J_{\text{AX}}=8.58$, $J_{\text{XX'}}=2.24$), 7.72 (m, 2H), 7.59 (AA'XX', 2H, $J_{\text{AX}}=8.72$, $J_{\text{XX'}}=2.31$), 7.39 (m, 2H), 7.33 (m, 1H), 6.99 (AA'XX', 2H, $J_{\text{AX}}=8.63$, $J_{\text{AA'}}=2.26$), 6.92 (AA'XX', 2H, $J_{\text{AX}}=8.68$, $J_{\text{AA'}}=2.67$), 3.88 (s, 3H), 3.85 (s, 3H); ^{13}C NMR (100 MHz, CDCl_3) δ 161.2, 159.9, 159.7, 145.1, 135.3, 132.9, 128.6 (2), 128.1 (2), 128.0 (2), 127.96 (2), 127.9, 121.7, 120.3, 114.2 (2), 114.1 (2), 55.4, 55.3; MS m/z 357.2 (M^+).

2,5-(4-Hydroxyphenyl)-4-phenyl oxazole (31). Oxazole **30** (22.0 mg, 0.062 mmol) was demethylated according to the general $\text{BF}_3\cdot\text{SMe}_2$ procedure above to give deprotected oxazole **31** as an off-white powder (18.1 mg, 89%). ^1H NMR (500 MHz, Acetone- d_6) δ 8.93 (br s, 1H), 8.77 (br s, 1H), 7.99 (AA'XX', 2H, $J_{\text{AX}}=8.83$, $J_{\text{XX'}}=2.41$), 7.72 (m, 2H), 7.53 (AA'XX', 2H, $J_{\text{AX}}=8.77$, $J_{\text{XX'}}=2.46$), 7.40 (m, 2H), 7.34 (tt, 1H, $J=7.36$, 1.33), 6.99 (AA'XX', 2H, $J_{\text{AX}}=8.70$, $J_{\text{AA'}}=2.40$), 6.92 (AA'XX', 2H, $J_{\text{AX}}=8.83$, $J_{\text{AA'}}=2.46$); MS m/z 329.1 (M^+); HRMS calc'd for $\text{C}_{21}\text{H}_{15}\text{NO}_3$: 329.1052, found 329.1055.

General procedure for pyrazole synthesis. A suspension of diketone (1 equiv) and appropriate hydrazine hydrochloride (3–5 equiv) in a 3:1 mixture DMF:THF was heated to reflux for 16–24 h with reaction progress being monitored by TLC for disappearance of starting material. The reaction mixtures was cooled to room temperature and poured into iced sat. LiCl solution (10 ml) and EtOAc (10 ml). The layers were separated and the organic layer was washed with brine (10 ml), dried over MgSO_4 , filtered and concentrated. Purification using flash column chromatography (EtOAc/hexanes systems) afforded the pyrazoles.

3,5-di(4-methoxyphenyl)-1H-pyrazole (34a). Diketone **33** (91 mg, 0.32 mmol) and hydrazine (0.1 ml, 3.2 mmol) were reacted as outlined in general pyrazole procedure to afford **34a** [45] as an off-white solid (32.6 mg, 38%). mp 172–175 $^\circ\text{C}$ (lit [45] mp 174 $^\circ\text{C}$); ^1H NMR (400 MHz, CDCl_3) δ 7.73 (AA'XX', 4H, $J_{\text{AX}}=8.73$, $J_{\text{AA'}}=2.42$), 6.97 (AA'XX', 4H, $J_{\text{AX}}=8.73$, $J_{\text{AA'}}=2.42$), 6.80 (s, 1H), 3.72 (s, 6H); ^{13}C NMR (100 MHz, CDCl_3) δ 159.9, 148.3, 126.8, 123.0, 112.9, 98.6, 54.5; MS (FAB) m/z (relative intensity, %) 281 (MH^+ , 100).

1-Phenyl-3,5-di(4-methoxyphenyl)-pyrazole (34b). Diketone **33** (100 mg, 0.35 mmol) and phenyl hydrazine hydrochloride (500 mg, 3.5 mmol) were reacted as outlined in general pyrazole procedure above to afford **34b** [46] (30 mg, 25%). mp 159–161 $^\circ\text{C}$ (lit [46] mp 163 $^\circ\text{C}$); ^1H NMR (400 MHz, CDCl_3) δ 7.82 (AA'XX', 2H, $J_{\text{AX}}=8.96$, $J_{\text{AA'}}=2.44$), 7.24–7.20 (m, 5H), 7.20 (AA'XX', 2H, $J_{\text{AX}}=8.79$, $J_{\text{AA'}}=2.46$), 6.99 (AA'XX', 2H, $J_{\text{AX}}=8.79$, $J_{\text{AA'}}=2.46$), 6.84 (AA'XX', 2H, $J_{\text{AX}}=8.96$, $J_{\text{AA'}}=2.44$), 6.70 (s, 1H), 3.84 (s, 3H), 3.80 (s, 3H); ^{13}C NMR (100 MHz, CDCl_3) δ 159.4, 151.5, 144.1, 140.0, 129.9, 128.8, 127.2, 126.9, 125.5, 125.2, 122.9, 113.9, 113.8, 104.1, 55.2, 55.1; MS (EI, 70 eV) m/z (relative intensity, %) 356 (M^+ , 100), 341 (19), 135 (89); HRMS calc'd for $\text{C}_{23}\text{H}_{20}\text{N}_2\text{O}_2$: 356.15241, found: 356.152478.

3,5-Di(4-hydroxyphenyl)-1H-pyrazole (35a). Pyrazole **34a** (20 mg, 0.07 mmol) was demethylated with BBr_3 according to the general procedure to afford **35a** [47] as an off-white solid (11 mg, 63%). ^1H NMR (400 MHz, Acetone- d_6) δ 8.58 (br s, 2H), 7.75 (AA'XX', 4H, $J_{\text{AX}}=8.95$, $J_{\text{AA'}}=2.46$), 6.93 (AA'XX', 4H, $J_{\text{AX}}=8.95$, $J_{\text{AA'}}=2.46$), 6.83 (s, 1H); ^{13}C NMR (100 MHz, Acetone- d_6) δ 157.1, 148.3, 126.5, 123.0, 115.3, 97.5; MS (CI, CH_4) m/z (relative intensity, %) 253.1 (MH^+ , 100), 237(10), 161 (5), 123 (15).

1-Phenyl-3,5-di(4-hydroxyphenyl)-pyrazole (35b). Pyrazole **34b** (20 mg, 0.06 mmol) was demethylated with BBr_3 according to the general procedure to afford **35b** [47] as an off-white solid (11.5 mg, 58%). ^1H NMR (400 MHz, CDCl_3) δ 8.64 (s, 1H), 8.45 (s, 1H), 7.79 (AA'XX', 4H, $J_{\text{AX}}=8.78$, $J_{\text{AA'}}=2.38$), 7.36 (m, 5H), 7.14 (AA'XX', 4H, $J_{\text{AX}}=8.60$, $J_{\text{AA'}}=2.47$), 6.90 (AA'XX', 2H, $J_{\text{AX}}=8.78$, $J_{\text{AA'}}=2.38$), 6.81 (AA'XX', 2H, $J_{\text{AX}}=8.78$, $J_{\text{AA'}}=2.47$), 6.80 (s, 1H); ^{13}C NMR (100 MHz, CDCl_3) δ 157.5, 157.3, 151.3, 144.1, 140.6, 129.9, 128.6, 126.8, 126.7, 124.9, 122.2, 122.1, 115.2, 115.1, 103.7; MS (EI, 70 eV) m/z (relative intensity, %) 362.1 (M^+ , 85), 328.1 (100).

4-Ethyl-3,5-di(4-methoxyphenyl)-1H-pyrazole (37a). Diketone **36** (100 mg, 0.32 mmol) and hydrazine (0.12 ml, 3.2 mmol) were reacted as outlined in the general pyrazole procedure above to afford **37a** as a white solid (69 mg, 70%). ^1H NMR (400 MHz, CDCl_3) δ 7.50 (AA'XX', 4H, $J_{\text{AX}}=8.84$, $J_{\text{AA'}}=2.48$), 6.94 (AA'XX', 4H, $J_{\text{AX}}=8.90$, $J_{\text{AA'}}=2.50$), 3.85 (s, 3H), 2.71 (q, 2H, $J=7.38$), 1.07 (t, 3H, $J=7.44$); ^{13}C NMR (100 MHz, CDCl_3) δ 159.4, 129.0, 127.4, 124.1, 116.8, 113.9, 55.1, 16.6, 15.3; MS (EI, 70 eV) m/z (relative intensity, %) 308.1 (M^+ , 100), 293.1 (73), 160.1 (7), 134 (8).

1-Phenyl-4-ethyl-3,5-di(4-methoxyphenyl)-pyrazole (37b). Diketone **36** (100 mg, 0.35 mmol) and phenyl hydrazine hydrochloride (140 mg, 0.96 mmol) were reacted as outlined in the general pyrazole procedure above to afford **37b** as an orange solid (109 mg, 87%). ^1H NMR (400 MHz, CDCl_3) δ 7.72 (AA'XX', 2H, $J_{\text{AX}}=9.03$, $J_{\text{AA'}}=2.44$), 7.24 (m, 3H), 7.20 (m, 2H), 7.17 (AA'XX', 2H, $J_{\text{AX}}=8.79$, $J_{\text{AA'}}=2.44$), 6.99 (AA'XX', 2H, $J_{\text{AX}}=8.79$, $J_{\text{AA'}}=2.56$), 6.90 (AA'XX', 2H, $J_{\text{AX}}=8.79$, $J_{\text{AA'}}=2.44$), 3.86 (s, 3H), 3.83 (s, 3H), 2.63 (q, 2H, $J=7.57$), 1.04 (t, 3H, $J=7.57$); ^{13}C NMR (100 MHz, CDCl_3) δ 159.6, 159.4, 150.8, 141.2, 140.5, 131.5, 129.3, 128.8, 127.0, 126.7, 124.8, 123.5, 120.7, 114.2, 114.1, 55.5, 55.4, 17.3, 15.8; MS (EI, 70 eV) m/z (relative intensity, %) 356 (M^+ , 100), 341 (100), 328 (15), 196 (25), 77 (40); HRMS calc'd for $\text{C}_{25}\text{H}_{24}\text{N}_2\text{O}_2$: 384.183582, found: 384.183778.

4-Ethyl-3,5-di(4-hydroxyphenyl)-1H-pyrazole (38a). Pyrazole **37a** (69 mg, 0.22 mmol) was demethylated according to the general BBr_3 procedure to afford **38a** as a white solid (35 mg, 57%). ^1H NMR (400 MHz, Acetone- d_6) δ 7.49 (AA'XX', 4H, $J_{\text{AX}}=8.85$, $J_{\text{AA'}}=2.46$), 6.93 (AA'XX', 4H, $J_{\text{AX}}=8.64$, $J_{\text{AA'}}=2.40$), 2.73 (q, 2H, $J=7.39$), 1.07 (t, 3H, $J=7.47$); ^{13}C NMR (100 MHz, Acetone- d_6) δ 156.9, 128.8, 124.3, 122.2, 115.4, 115.2, 16.5, 14.9; MS (CI, CH_4) m/z (relative intensity, %) 282.1 ($\text{M}+\text{H}^+$, 100), 263.1 (10), 187.1 (20).

1-Phenyl-4-ethyl-3,5-di(4-hydroxyphenyl)-pyrazole (38b). Pyrazole **37b** (100 mg, 0.26 mmol) was demethylated according to the general BBr_3 procedure to afford **38b** as a white solid (50 mg, 54%). ^1H NMR

(400 MHz, MeOH- d_4) δ 7.51 (AA'XX', 4H, J_{AX} = 8.67, J_{AA} = 2.47), 7.24–7.42 (m, 5H), 7.05 (AA'XX', 4H, J_{AX} = 8.81, J_{AA} = 2.40), 6.88 (AA'XX', 2H, J_{AX} = 8.67, J_{AA} = 2.46), 6.78 (AA'XX', 2H, J_{AX} = 8.81, J_{AA} = 2.40), 2.60 (q, 2H, J = 7.53), 0.98 (t, 3H, J = 7.39); MS (EI, 70 eV) m/z (relative intensity, %) 356.1 (M^+ , 100), 341.1 (100), 328.1 (15), 196.1 (25), 77 (40); HRMS calc'd for $C_{23}H_{21}N_2O_2$: 357.161155, found: 357.160303.

3,5-Di(4-methoxyphenyl)isoxazole (40). To a solution of oxime **39** (1.0 g, 6 mmol) in THF (20 mL) at 0°C was added $n\text{BuLi}$ (9.11 mL, 13.3 mmol) as a solution in hexanes. The clear solution was stirred for 30 min at 0°C then methyl 4-methoxybenzoate (498 mg, 3 mmol) was added as a solution in THF (5 mL) over 5 min. The reaction mixture was stirred at 0°C for 30 min, then warmed to room temperature. 5 N HCl (10 mL) was added and the biphasic reaction mixture was brought to reflux overnight (12 h). Upon cooling to 0°C, isoxazole **40** precipitated [33] and was collected via filtration (450 mg, 27%). mp 174–177°C (lit [33] mp 176–177°C); ^1H NMR (400 MHz, Acetone- d_6) δ 7.66 (AA'XX', 2H, J_{AX} = 8.88, J_{AA} = 2.44), 7.63 (AA'XX', 2H, J_{AX} = 9.1, J_{AA} = 2.15), 6.86 (AA'XX', 2H, J_{AX} = 8.88, J_{AA} = 2.44), 6.85 (AA'XX', 2H, J_{AX} = 9.1, J_{AA} = 2.44), 6.57 (s, 1H), 3.73 (s, 3H), 3.72 (s, 3H); ^{13}C NMR (100 MHz, Acetone- d_6) δ 169.8, 162.3, 160.8, 160.7, 127.9, 127.1, 121.5, 120.0, 114.1, 114.0, 95.7, 55.1, 55.0; MS (EI, 70 eV) m/z (relative intensity, %) 281.1 (M^+ , 5), 150.1 (20), 135.1 (100).

3,5-Di(4-hydroxyphenyl)isoxazole (41). Isoxazole **40** (300 g, 1.1 mmol) was demethylated according to the general BBr_3 procedure to afford **41** [34] as a white solid (152 mg, 56%). mp 267–269°C (lit [34] mp 255°C); ^1H NMR (400 MHz, Acetone- d_6) δ 10.07 (s, 1H), 9.91 (s, 1H), 7.90 (d, 4H, J = 8.79), 7.21 (s, 1H), 6.88 (4H, t, J = 9.38); ^{13}C NMR (100 MHz, MeOH- d_4) δ 170.3, 162.8, 159.1, 127.7, 126.9, 119.9, 118.7, 116.3, 115.1, 95.3, 95.0; MS (EI, 70 eV) m/z (relative intensity, %) 253.1 (M^+ , 60), 133.1 (25), 121.1 (100), 93.0 (20), 77.0 (10), 65.0 (30).

Supplementary material available

Experimental detail regarding the preparation of all intermediates discussed in the synthesis of the above heterocycles is available with the online version of this paper.

Acknowledgements

We are grateful for support of this research through grants from the National Institutes of Health (PHS 5R37 DK15556) and the U.S. Army Breast Cancer Research Program (DAMD17-97-1-7076). We thank Kathryn Carlson for determining estrogen receptor binding affinities. NMR spectra were obtained in the Varian Oxford Instrument Center for Excellence in NMR Laboratory. Funding for this instrumentation was provided in part from the W.M. Keck Foundation, the National Institutes of Health (PHS 1 S10 RR104444-01) and the National Science Foundation (NSF CHE 96-10502). Mass spectra were obtained on instruments supported by grants from the National Institute of General Medical Sciences (GM 27029), the National Institutes of Health (RR 01575), and the National Science Foundation (PCM 8121494).

References

- Grese, T.A., et al., & Dodge, J.A. (1997). Molecular determinants of tissue selectivity in estrogen receptor modulators. *Proc. Natl Acad. Sci. USA* **94**, 14105-14110.
- Kuiper, G.G.J.M., Enmark, E., Peltö-Huikko, M., Nilsson, S. & Gustafsson, J.Å. (1996). Cloning of a novel receptor expressed in rat prostate and ovary. *Proc. Natl Acad. Sci. USA* **93**, 5925-5930.
- Mosselman, S., Polman, J. & Dijkema, R. (1996). ER β : Identification and characterization of a novel human estrogen receptor. *FEBS Lett.* **392**, 49-53.
- Katzenellenbogen, J.A. & Katzenellenbogen, B.S. (1996). Nuclear hormone receptors: ligand-activated regulators of transcription and diverse cell responses. *Chem. Biol.* **3**, 529-536.
- Horwitz, K.B., et al., & Tung, L. (1996). Nuclear receptor coactivators and corepressors. *Mol. Endocrinol.* **10**, 1167-1177.
- Glass, C.K., Rose, D.W. & Rosenfeld, M.G. (1997). Nuclear receptor coactivators. *Curr. Opin. Cell. Biol.* **9**, 222-232.
- Katzenellenbogen, J.A., O'Malley, B.W. & Katzenellenbogen, B.S. (1996). Tripartite steroid hormone receptor pharmacology: interaction with multiple effector sites as a basis for the cell- and promoter-specific action of these hormones. *Mol. Endocrinol.* **10**, 119-131.
- Magarian, R.A., Overacre, L.B. & Singh, S. (1994). The medicinal chemistry of nonsteroidal antiestrogens: a review. *Curr. Med. Chem.* **1**, 61-104.
- Grundy, J. (1957). Artificial estrogens. *Chem. Rev.* **57**, 281-416.
- Solmsen, U.V. (1945). Synthetic estrogens and the relation between their structure and their activity. *Chem. Rev.* **37**, 481-598.
- Grese, T.A., et al., & Bryant, H.U. (1998). Synthesis and pharmacology of conformationally restricted raloxifene analogues: highly potent selective estrogen receptor modulators. *J. Med. Chem.* **41**, 1272-1283.
- Plakowicz, A.D., et al., & Bryant, H.U. (1997). Discovery and synthesis of [6-Hydroxy-3-[4-[2-(1-piperidinyl)ethoxy]phenoxy]-2-(hydroxyphenyl)]benzo[b]thiophene: a novel, highly potent, selective estrogen receptor modulator. *J. Med. Chem.* **40**, 1407-1416.
- Brown, D.S. & Armstrong, R.W. (1996). Synthesis of tetra-substituted ethylenes on solid support via resin capture. *J. Am. Chem. Soc.* **118**, 6331-6332.
- Williard, R., et al., & Scanlan, T.S. (1995). Screening and characterization of estrogenic activity from hydroxystilbene library. *Curr. Biol.* **2**, 45-51.
- Sarshar, S., Siev, D. & Mjalli, A.M.M. (1996). Imidazole libraries on solid support. *Tetrahedron Lett.* **37**, 835-838.
- Bredereck, H., Gompper, R. & Hayer, D. (1959). Imidazole aus α -diketonen. *Chem. Ber.* **92**, 338-343.
- Lombardino, J.G. & Weisman, E.H. (1974). Preparation and antiinflammatory activity of some nonacidic trisubstituted imidazoles. *J. Med. Chem.* **17**, 1182-1188.
- Schubert, V.H., Giesemann, G., Steffen, P. & Bleichert, J. (1962). p-Aryl- und p-Alkoxyphenyl-imidazole. *J. Prakt. Chem.* **18**, 192-202.
- Hayes, J.F., Mitchell, M.B. & Wicks, C. (1994). A novel synthesis of 2,4,5-triarylimidazoles. *Heterocycles* **38**, 575-585.
- Gardner, P.D. (1956). Organic peracid oxidation of some enol esters involving R' rearrangement. *J. Am. Chem. Soc.* **78**, 3421-3424.
- Jenkins, S.S. (1934). The grignard reaction in the synthesis of ketones. IV. A new method of preparing isomeric unsymmetrical benzoin. *J. Am. Chem. Soc.* **56**, 682-684.
- Patonay, T. & Hoffman, R.V. (1995). Base-promoted reactions of α -azido ketones with aldehydes and ketones: a novel entry to α -azido-hydroxy ketones and 2,5-dihydro-5-hydroxyoxazoles. *J. Org. Chem.* **60**, 2368-2377.
- Taylor, E.C. & Zoltewicz, J.A. (1960). A new synthesis of aliphatic and aromatic thioamides from nitriles. *J. Am. Chem. Soc.* **82**, 2656-2657.
- Dolling, K., Zschke, H. & Schubert, H. (1979). Kristallin-flüssige Thiazole. [Liquid-crystalline thiazoles.] *J. Prakt. Chem.* **321**, 643-654.
- Katritzky, A.R., Boulton, A.J. & Short, D.J. (1960). Interaction at a distance in conjugated systems. Part III. Effect of aryl and heteroaryl groups on the infrared intensities of C=C and C-C stretching bands. *J. Chem. Soc.* 1519-1523.
- Cowper, R.M. & Stevens, T.S. (1940). Mechanism of the reaction between arylamines and benzoin. *J. Chem. Soc.* 347-349.
- Strzybny, P.P.E., van ES, T. & Backeberg, O.G. (1969). Reaction of α -acyloxyketones with ammonium acetate. *J. South African Chem. Inst.* **22**, 158-164.
- Marzinzik, A.L. & Felder, E.R. (1996). Solid support synthesis of highly functionalized pyrazoles and isoxazoles: scaffolds for molecular diversity. *Tetrahedron Lett.* **37**, 1003-1006.
- Reitz, D.B., Beak, P., Farney, R.F. & Helmick, L.S. (1978). Dipole-stabilized carbanions from thioesters. Evidence for stabilization by the carbonyl group. *J. Am. Chem. Soc.* **100**, 5428-5436.
- Tewari, S.C. & Rastogi, S.N. (1979). Studies in antifertility agents: Part XXII: 1,2-diethyl-1,3-bis-(p-hydroxyphenyl)-1-propene. *Ind. J. Chem.* **18B**, 62-64.
- Clark, J.H. & Miller, J.M. (1977). Hydrogen bonding in organic synthesis. Part 6. C-Alkylation of β -dicarbonyl compounds using tetraalkylammonium fluorides. *J. Chem. Soc., Perkin I*, 1743-1745.
- Perkins, M., Beam, C.F., Dyer, M.C.D. & Hauser, C.R. (1988). 3-(4-Chlorophenyl)-5-(4-methoxyphenyl)isoxazole. *Org. Syn. Coll. Vol.* **VI**, 278-281.
- Ichinose, N., Mizuno, K., Tami, T. & Otsuji, Y. (1988). A novel NO insertion into cyclopropane ring by use of NOBF $_4$. Formation of 2-isoxazolines. *Chem. Lett.*, 233-236.
- Murthy, A.K., Rao, K.S.R.K.M. & Rao, N.V.S. (1968). Isoxazolyphenols and their absorption spectra. *Aus. J. Chem.* **21**, 2315-2317.
- Katzenellenbogen, J.A., Myers, H.N., Johnson, H.J., Jr, Kempton, R.J. & Carlson, K.E. (1977). Estrogen photoaffinity labels. 1. Chemical and radiochemical synthesis of hexestrol diazoketone and azide derivatives; photochemical studies in solution. *Biochemistry* **16**, 1964-1970.

36. Anstead, G.M., Carlson, K.E. & Katzenellenbogen, J.A. (1997). The estradiol pharmacophore: ligand structure-estrogen receptor binding affinity relationships and a model for the receptor binding site. *Steroids* **62**, 268-303.
37. von Angerer, E., Prekajac, J. & Strohmeier, J. (1984). 2-Phenylindoles. Relationship between structure, estrogen receptor affinity, and mammary tumor inhibiting activity in the rat. *J. Med. Chem.* **27**, 1439-1447.
38. Hwang, K.J., O'Neil, J.P. & Katzenellenbogen, J.A. (1992). 5,6,11,12-Tetrahydrochrysenes: Synthesis of rigid stilbene systems designed to be fluorescent ligands for the estrogen receptor. *J. Org. Chem.* **57**, 1262-1271.
39. Joule, J.A., Mills, K. & Smith, G.F.J. (1995). *Heterocyclic Chemistry*. Third ed. p 516, Chapman and Hall, New York.
40. von Angerer, E. & Erber, S. (1992). 3-Alkyl-2-phenylbenzo[b]thiophenes: nonsteroidal estrogen antagonists with mammary tumor inhibiting activity. *J. Steroid Biochem. Mol. Biol.* **41**, 557-562.
41. Grese, T.A., *et al.*, & Sata, M. (1996). Benzopyran selective estrogen receptor modulators (SERMS): Pharmacological effects and structural correlation with raloxifene. *Bioorg. Med. Chem. Lett.* **6**, 903-908.
42. Brzozowski, A.M., *et al.* & Carlquist, M. (1997). Molecular basis of agonism and antagonism in the oestrogen receptor. *Nature* **389**, 753-758.
43. Sun, J., *et al.*, & Katzenellenbogen, B.S. (1999). Novel ligands that function as selective estrogens or antiestrogens for estrogen receptor- α or estrogen receptor- β . *Endocrinology*, **140**, 800-804.
44. Katzenellenbogen, J.A., Johnson, H.J. & Myers, H.N. (1973). Photoaffinity labels for estrogen binding proteins of rat uterus. *Biochemistry* **12**, 4085-4092.
45. van Steenis, J. (1946). The nitration of dianisoylmethane and p-methoxydesoxybenzoin. *Recl. Trav. Chim. Pays-Bas* **66**, 29-46.
46. Ando, W., Sato, R., Yamashita, M., Akasaka, T. & Miyazaki, H. (1983). Quenching of singlet oxygen by 1,3,5-triaryl-2-pyrazolines. *J. Org. Chem.* **48**, 542-546.
47. Hergenrother, P.M. (1991). New developments in thermally stable polymers. *Rec. Trav. Chim. Pays-Bas*. **110**, 481-491.